

# CORRELATION ANALYSIS OF MODAL ANALYSIS RESULTS FROM A PIPELINE

Heikki Haapaniemi<sup>1)</sup>, Pekka Luukkanen<sup>2)</sup>, Pekka Nurkkala<sup>3)</sup>, Jaakko Rostedt<sup>4)</sup> and Arja Saarenheimo<sup>1)</sup>

1) VTT Industrial Systems P.O.Box 1704, FIN-02044 VTT, Finland

2) Fortum Power and Heat Ltd LOVIISA NPP P.O.Box 23, 07901 Loviisa, Finland

3) Fortum Energy Solutions Ltd P.O.Box 20, 00048 FORTUM, Finland

4) J. Rostedt Ltd, Harjukatu 18, 38710 Kankaanpää, Finland

## ABSTRACT

The main objective of this ongoing project is to develop practical methods for monitoring the condition and remaining lifetime of process piping. The project consists of several different tasks: finite element (FE) modelling, pre-test analysis, modal testing, modal correlation analysis and model updating. This paper is focused on correlation analysis between test results of one pipeline in different boundary conditions and also on correlation analysis between traditional impact hammer and shaker excitation test results. Correlation was also analysed between results from the so-called output-only modal analysis and shaker tests. Special interest is laid on the verification of the output-only modal analysis techniques, because it may offer a possibility to obtain modal parameters of a piping system even when then system is in use.

## NOMENCLATURE

$\alpha$	frequency response function
$\omega$	circular frequency (1/s)
$\Psi$	eigenvector
$\chi$	common coordinate

## 1 INTRODUCTION

Dynamic behaviour of the feed water pipeline RL61 of the VVER 440 type PWR nuclear power plant Loviisa 1 were studied by modal testing and using numerical methods. Modal testing with impact hammer and shaker excitation was performed during the outage in autumn

2001 and operational measurements were performed during summer of 2002. The pipeline was tested first as non-insulated, cold and empty (Case 1). In the second case (Case 2) the insulation was added and in the third case (Case 3) the pipe was filled with hot water (165°C). Impact hammer tests were done in the boundary conditions (BC) referred as Case 1 and operational measurements were done in BCs referred as Case 3. Shaker tests were done using two exciter directions.

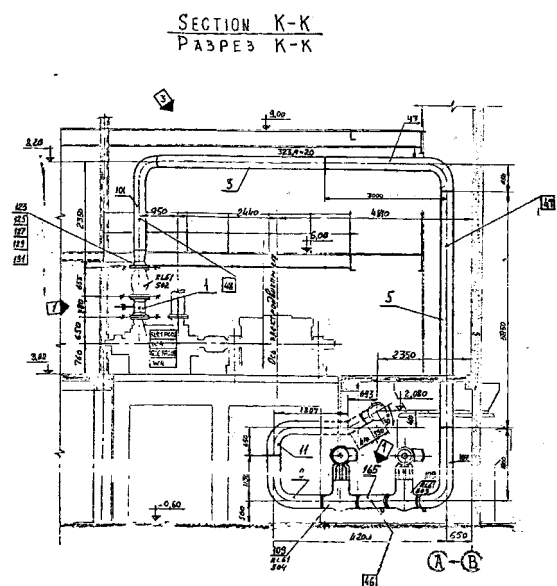


Figure 1. Feed water line RL61.

The output only measurements were carried out in operational conditions (pressure 7.5 MPa) BCs corresponding other wise Case 3.

The main dimensions of the pipeline are shown in Fig. 1. The outer radius of the pipe is 324 mm and the pipe bend curvature 600mm. The thickness of the pipe is generally 20 mm, except for the longest vertical part, which has a wall thickness of 17.5 mm.

## 2 PRE-TEST ANALYSIS

Pre-test analyses were carried out using the FEMtools program [1]. The optimal locations for excitation of the structure were identified. Also, the numerically predicted mode shapes can be used to select the optimal minimum set of DOF (Degrees Of Freedom) where measurements are required to enable pairing with calculated mode shapes. The ABAQUS/Standard [2] code was used for finite element analyses.

Driving point residues (DPR) are equivalent to modal participation factors. They are proportional to the magnitudes of the resonance peaks when measuring FRF at a driving point. A driving point is defined as any point in the structure where the excitation DOF and the response DOF are equal. A shaker or a reference accelerometer is usually located at a driving point. The driving point residues for all the DOFs in a FE model can be computed as

$$DPR_j(i, i) = \frac{\Psi_j(i)^2}{\omega_j} \quad (1)$$

where  $i$  is the degree of freedom,  $\psi$  the eigenvector,  $\omega$  the circular frequency, and  $j$  the mode shape number. DPRs are a measure of how much each mode is excited, or has participated in the overall response, at the DPR [3].

The driving point residues are normalised and compared with a range of mode shapes of interest. The Normalised Modal Displacement (NMD) is used as a criterion and can be calculated using minimum, maximum, averaged maximum or combined weighted maximum and averaged maximum values. In order to get the best point and direction for exciting, the case in which the DPRs for all modes of interest are as high as possible should be chosen. In a case where excitation of certain modes is unfavourable, the driving point should be chosen with the minimal DPRs for those modes.

A certain minimum number of DOFs is needed in a FE model to obtain sufficient accuracy of results. Also, there is a minimum number of test DOFs needed to model the mode shapes and to distinguish one mode shape from another.

In this study, the optimal exciter locations for RL61 measurements were predicted using weighted NMDs, which are defined as follows:

$$NMD(i) = [\max_{j=1}^M (\overline{DPR}_j(i, i))] [\frac{1}{M} \sum_{j=1}^M (\overline{DPR}_j(i, i))] \quad (2)$$

where  $M$  is the number of mode shapes of interest [1].

The pipeline was modelled with straight pipe elements of type PIPE31 and special purpose pipe bend elements of type ELBOW31, which allow cross-sectional ovalisation

and warping, where as the PIPE31 type beam element expands only radially. There are six elbow elements modelling one pipe bend of 90 degrees. All elbow elements used in the analyses incorporate six circumferential Fouries modes for ovalisation, seven integration points through the wall thickness, one integration point in the axial direction and 18 circumferential integration points.

In this preliminary study, the connection to the pump and the downstream end of the model were modelled as fully fixed. This pipeline is supported by three spring hangers. The locations of the spring hangers referred to in the following as S1, S2 and S3 are shown in Fig.1 numbered 46, 47 and 48, respectively. The spring constant of S1 is 660 N/mm and the corresponding value for springs S2 and S3 is 446N/mm. There are two valves, V1 and V2, each weighing 978 kg.

First, the pipe was assumed to be non-insulated, cold and empty. The summarised NMD values in relation to the global X-, Y- and Z-axes are shown as vectors in Fig. 2. The NMDs were calculated also assuming that the pipeline is filled with water, but non-insulated and cold. The mass of the water was included in the equivalent density of the pipe cross-section. The corresponding vector plot essentially resembles the one shown in Fig. 2. This result was used in choosing the excitation location.

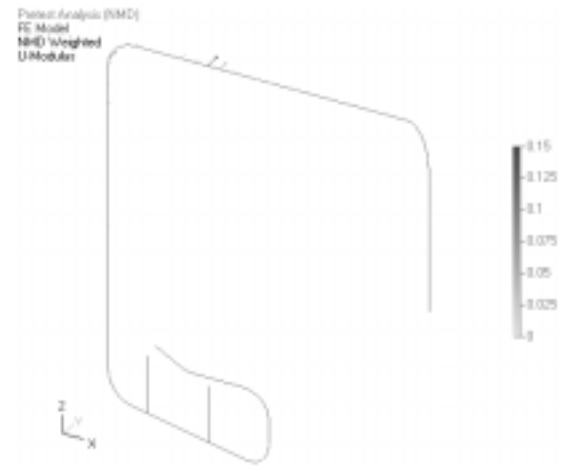


**Figure 2.** Modulus of weighted NMDs.

The Modal Assurance Criteria (MAC) was used in selecting the locations for transducers. MAC evaluates the correlation between two different mode shapes  $\{\psi_1\}$  and  $\{\psi_2\}$  numerically. These mode shapes can be either measured or analytical ones. The following equation is used to evaluate MAC values:

$$MAC(\psi_1, \psi_2) = \frac{\left| \left( \{\psi_1\}^T \{\psi_2\} \right) \right|^2}{\left( \{\psi_1\}^T \{\psi_1\} \right) \left( \{\psi_2\}^T \{\psi_2\} \right)} \quad (3)$$

In general a higher MAC value indicates better correlation between modes i.e. two mode shapes with 100% correlation represents perfect correlation.

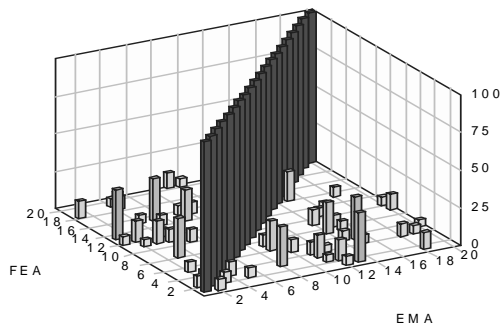


**Figure 3.** MAC matrix of measurement point selection.

The analytical mode shapes are compared with the truncated test mode shapes using Eq. (3). Truncated test mode shapes are created by truncating analytical modes so that they correspond to the selected measurement locations. The correlation results in MAC matrix form for the measurement point selection is presented in Fig. 3. The model used in modal testing and the locations and numbers of measurement points are shown in Fig. 4.

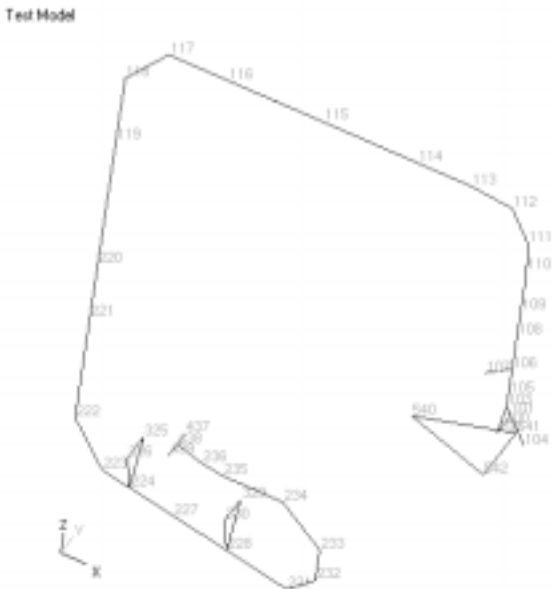


**Figure 4.** Measurement points.

### 3 SHAKER TESTS

Modal testing with shaker excitation was performed during the outage [4]. The responses were measured at all the measurement points to all the three global co-

ordinate directions, which are also shown in Fig. 4. For practical reasons excitation at point 114 was done in the global negative Z-axis and global negative Y-axis directions. In the following these excitation points are referred to as 114Y- and 114Z-. The excitation was given in one direction at a time. A servo-hydraulic exciter was used for excitation. The mass of the exciter was 400 kg and maximum nominal dynamic force 11 kN. The choice of frequency range was based on the pre-analyses and the number of available transducers. The frequency range used in these measurements was 0...100 Hz.

**Table 1.** Natural frequencies with shaker excitation (114Y-).

Mode	Case 1 (Hz)	Case 2 (Hz)	Case 3 (Hz)
1	1.812	3.118	4.279
2	3.594	4.412	6.833
3	4.718	4.921	9.175
4	5.599	5.673	9.339
5	6.551	6.634	11.431
6	6.68	6.934	20.124
7	9.572	9.441	20.634
8	11.67	11.261	23.64
9	14.272	11.629	24.732
10	17.451	20.914	24.89
11	18.961	21.067	37.994
12	21.4	24.603	39.778
13	21.672	25.311	
14	25.384	25.64	
15	25.986	26.091	
16	29.544	29.224	
17	39.07		
18	41.6		
19	42.109		
20	47.418		
21	49.539		
22	55.087		
23	55.526		
24	65.322		
25	66.118		
26	67.255		

Frequency response functions (FRFs) were measured with 16 channel Brüer & Kjaer IDA signal analyser and SRDC IDEAS-MS6 software. With this set-up it was possible to measure 15 FRFs simultaneously (15 response channels and one reference channel).

Modal analysis was performed with SRDC IDEAS-MS7 software [5] using the Complex Exponential method for solving natural frequencies and damping values and Circle-Fit algorithm for solving mode shapes [4]. Resulting natural modes for all three different BC cases (Case 1, Case 2 and Case 3) when excitation was given at point 114Y- are shown in Table 1.

Damping values varied between 0.5% to 2.9% (Case 1), 0.5% to 10.2% (Case 2) and 0.5% to 3.0% (Case 3).

#### 4 IMPACT HAMMER TESTS

In the non-insulated case (Case 1) modal testing was done also using an impact hammer [6]. The weight of the hammer is 22.3 kg. The hammer impact was given at point 114, to the global Y-direction. It should be noted that only points 114 to 228 and points 325 and 326 were measured (see Fig. 4). In all points the vibrations were measured in three global directions.

No curve fitting method was used; the eigenfrequencies were determined by visual investigation of the frequency-response-functions. Resulting natural frequencies are listed in Table 2.

**Table 2.** Natural frequencies with impact hammer excitation, Case 1.

Mode	1	2	3	4	5
(Hz)	2.0	3.75	7.125	9.75	11.975
Mode	6	7	8	9	10
(Hz)	19.25	21.50	26.50	39.125	43.375
Mode	11	12	13	14	15
(Hz)	44.375	50.75	56.75	69.125	76.875

#### 5 OUTPUT-ONLY MODAL ANALYSIS

Time history data recording for the output-only modal analysis was carried out using similar measurement configuration as during normal shaker tests. Point 114Y- was used as reference co-ordinate and measurement data was collected from 31 measurement DOFs. Because operational deflection shapes were measured at the same time five measurement runs was needed in order to complete these time history recordings. This resulted in five time history data sets.

One important factor is that the output only modal analysis reveals especially those natural modes, which are actually excited during operational use. Length of each measured time series is 576 seconds, the used sampling interval was 15.63 ms and the sampling frequency was set to 64 Hz. This means that each data set has 36864 samples and their size varies between 3844 Kbytes and 13454 Kbytes depending on number of measured DOFs in a data set.

Output-only modal analysis was carried out by using the ARTeMIS Extractor Pro code [7]. The used method is based on the Frequency Domain Decomposition (FDD) technique. The power spectral density function matrices are decomposed using singular value decomposition. Theoretical background is presented in detail in [8].

Several different tools such as magnitudes and coherence of the estimated spectral density functions between two different measured DOFs, singular values of the matrices of the estimated spectral density functions (SVDs) and average values of the elements of each of the matrices of the estimated spectral density functions were used for modal identification.

Magnitudes of some of the estimated spectral density functions between two different measured DOFs are presented in Fig. 5. Here the presented DOF pairs are 114Y- and 235Y+, 114Y- and 542Y- and 114Y- and 110Y+. These DOF pairs indicate peaks and possible natural frequencies at frequencies between 4.3 and 4.5 Hz (pairs 114Y-/110Y+ and 114Y-/235Y+), about 6.8 Hz (all three pairs) and about 9.1 Hz (all three pairs).

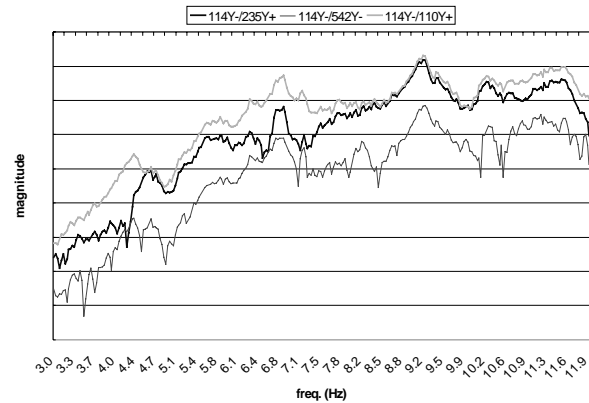


**Figure 5.** Magnitudes of the estimated spectral density functions between different measured DOFs.

The coherence function can be used for finding natural frequencies in a case of output only measurements because it obtains high values at frequencies, where a strong vibration pattern exist and high signal to noise ratio is found (except at nodal points) i.e. at resonance frequencies. Coherence of the estimated spectral density functions between two different measured DOFs in case of DOF pairs 114Y- and 222Y+ and 114Y- and 223Y+ is shown in Fig. 6. This figure shows that with these DOF high coherence can be found at frequencies about 4.3 Hz, 5.5 Hz, 9.2. Hz and between 10.5 and 11.7 Hz. With DOF pair 114Y- and 222Y+ there is also high coherence at about 6.8 Hz.

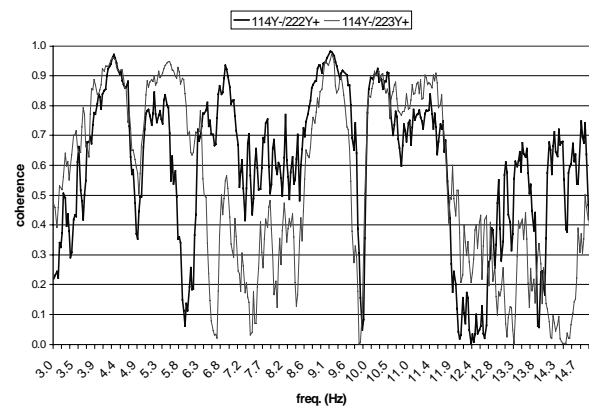


**Figure 6.** Coherence of the estimated spectral density functions between different measured DOFs.

Average values for all elements of each of the matrices of all the estimated spectral density functions are presented in Fig. 7. These average lines provide an indication of where the most dominating modes are located and what their energy levels are. Clear peaks can be found at frequencies about 4.3 Hz, 6.8 Hz and 9.2 Hz. High values can also be found at frequencies between 11.3 and 11.6 Hz.

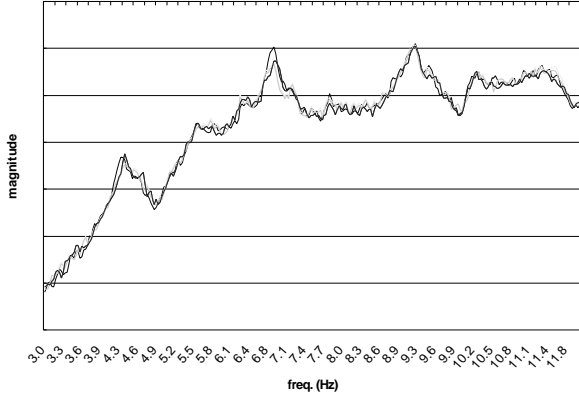


**Figure 7.** Averages of all elements of each of the matrices of the estimated spectral density functions.

According to the information obtained with above-mentioned tools modal identification was performed with the FDD technique at frequencies about 4.3 Hz, 6.8 Hz, 9.2 Hz and also all frequencies between 11 Hz and 12 Hz were carefully studied. Resulting natural frequencies are shown in Table 3.

**Table 3.** Natural frequencies with output only modal analysis and the FDD technique, Case 3.

Mode #	1	2	3	4	5
Frequency [Hz]	4.34	6.84	9.19	9.22	11.66

## 6 CORRELATION ANALYSIS TOOLS

Modal analysis results obtained using these above mentioned three different measurement methods were evaluated using four major correlation criteria: the frequency error, the Modal Assurance Criteria (MAC), the Cross Signature Assurance Criterion (CSAC), the Cross Signature Scale Factor (CSF) and the Coordinate Modal Assurance Criterion (COMAC). All correlation analyses were performed using FEMtools modal correlation and model updating software [1].

Frequency error simply indicates the percentual difference between found natural frequencies of two different measurement set-ups, BC set-ups or experimental and FE-model.

The following interpretation has been suggested [9] for the MAC: a value less than 5% indicates non-correlated mode shapes and a value higher than 90% correlated mode shapes. In real life situation a MAC values below 50% may indicate poor correlation and values above 70% good correlation.

Both CSAC and CSF were used to directly correlate frequency response functions (FRFs) over a frequency range. One major advantage of this approach is that no

modal analysis of the measured FRFs is required and identification errors are thus avoided [10].

The CSAC is one measure of correlation, similar to the MAC, between different FRFs in the frequency domain. At each frequency point  $\omega_k$ , the level of correlation between all corresponding experimental FRFs ( $\alpha_e$ ) and predicted FRFs ( $\alpha_a$ ) is evaluated as:

$$CSAC(\omega_k) = \frac{|\alpha_{1_i}^H(\omega_k) \alpha_{2_i}(\omega_k)|^2}{(\alpha_{1_i}^H(\omega_k) \alpha_{1_i}(\omega_k))(\alpha_{2_i}^H(\omega_k) \alpha_{2_i}(\omega_k))} \quad (4)$$

where  $\omega_k$  is the frequency at point k. The frequency range considered is divided into a certain number of frequency points (Nf);  $k=1,2,\dots,Nf$ . In this study, ( $\alpha_1$ ) is the measured FRF in Case 1, and ( $\alpha_2$ ) is the measured FRF in Case 2 (insulated). Subscript i is the number of DOFs in the system considered. Values for the CSAC ranges from 0 to 1 (or 0% to 100%) and higher values indicate better correlation over a certain frequency range. Superscript H stands for the Hermitian transpose.

Because CSAC evaluates the shape correlation of the FRFs, which is mainly determined by the position and amount of resonance peaks, this function is most sensitive to differences in mass and stiffness of different experimental (or analytical) models.

Because an FRF is not only defined by its shape it is necessary to apply another correlation function which evaluates the discrepancies between amplitudes of different FRFs and is very similar to the modal scale factor (MSF). The CSF function is defined as

$$CSF(\omega_k) = \frac{2|\alpha_{1_i}^H(\omega_k) \alpha_{2_i}(\omega_k)|}{(\alpha_{1_i}^H(\omega_k) \alpha_{1_i}(\omega_k)) + (\alpha_{2_i}^H(\omega_k) \alpha_{2_i}(\omega_k))} \quad (5)$$

Like the CSAC, the CSF is defined at each frequency point  $\omega_k$  and its value ranges from 0 to 1 (or 0% to 100%) with higher values indicating better correlation over certain frequency range. Because CSF evaluates amplitudes, this function is more sensitive to changes of damping.

The COMAC is a correlation indicator corresponding to a given common coordinate  $\chi$  between the considered results and it is used to quantify the correlation of modal displacement. The COMAC value is calculated for each DOF i

$$COMAC_i = \frac{\sum_{r=1}^L |({}^i\chi_{1r})({}^i\chi_{2r})|^2}{\sum_{r=1}^L ({}^i\chi_{1r})^2 \sum_{r=1}^L ({}^i\chi_{2r})^2} \quad (6)$$

where L is the number of well-correlated modes, Superscript i is number of DOF and subscripts 1 and 2 refer to the modes to be compared with each other. A value close to 1 suggests a good correlation.

## 7 CORRELATION BETWEEN SHAKER AND IMPACT HAMMER TEST RESULTS

Correlation between shaker and impact hammer test results in Case 1 was evaluated by both comparing the natural frequencies and by evaluating FRF correlation in

a frequency domain using correlation functions such as CSAC and CSF.

Natural mode and frequency comparison shown in Fig. 8 indicates that the two lowest modes have similar frequencies but above that it seems that shaker excitation have excited more modes than impact hammer excitation, which can also be confirmed by comparing tables 1 and 2. Fig. 8 also indicates that several of these modes have close frequencies like in case of impact hammer mode number 4 and shaker test mode 7 or impact hammer mode number 5 and shaker test mode 8. On the other hand impact tests have not excited any modes at frequency range from 12 Hz to 19 Hz while shaker tests show three modes in this frequency range. Though it must be remembered that during the impact hammer tests only a part of the piping system were measured and this may be an explanation for at least some of discrepancy in the number of found modes.

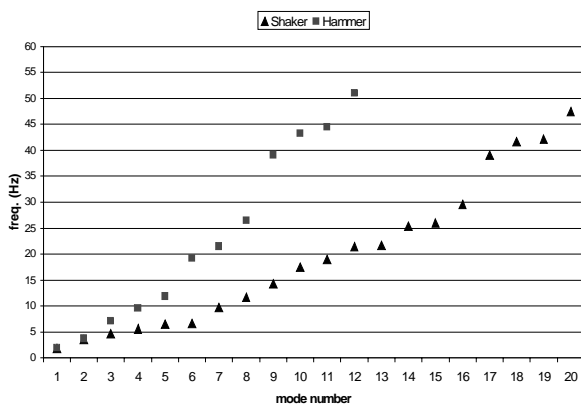


**Figure 8.** Natural mode and frequency comparison of modes below 60 Hz.

FRF correlation analysis results are presented in Figs 9 and 10. The correlation evaluated using all possible DOF pairs is referred as ALL curve. Corresponding result using only pairs from upper part of the piping (points from 114 to 220) is referred as TOP curve and correlation result for pairs from lower part of the piping (points from 220 to 228 and points 325 and 326) is referred as BOTTOM curve.

CSAC analysis results shown in Fig. 9 indicate good correlation for all FRF sets frequencies between 2 Hz and 9.75 Hz. Sharp valleys are probably caused by slight differences in natural frequencies i.e. at locations of FRF peaks or by lack of some modes at this frequency range in impact hammer FRFs. Correlation is low in frequencies between 11.75 Hz 22 Hz for all FRF sets as expected, except for a few peaks at frequencies about 19 Hz and 21 Hz. Above 22 Hz correlation is good in the case of FRF sets ALL and TOP. In general, the correlation seems to be better at the upper part of the piping than at the lower part. This may be caused by the lower excitation energy levels during impact hammer testing and the lower part of the piping with the massive valves was not properly excited.

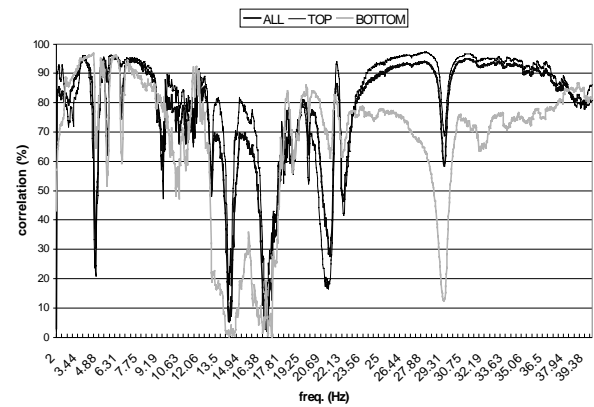


**Figure 9.** CSAC analysis results.

CSF analysis results in Fig. 10 show clear discrepancy in the amplitudes of the measured FRFs. No particular reason for this could be established but one explanation may be in the difference of used energy levels and high damping values (from 0.5% to 2.9%) even in the empty non-insulated piping.

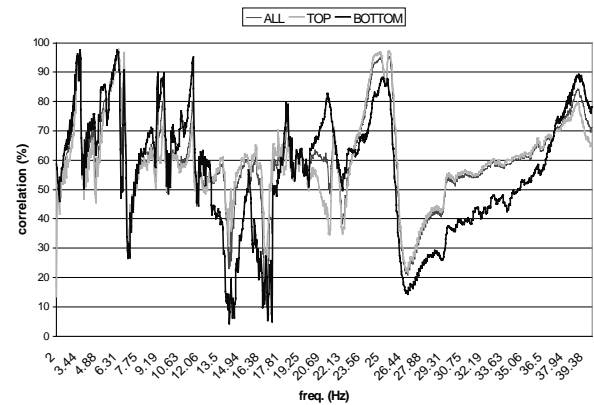


**Figure 10.** CSF analysis results.

In general, these results show that there is good correlation between impact hammer test results and shaker test results at lower frequencies. Also correlation seem to be better in areas closer to the excitation point, in this case at the upper part of the piping system, than in areas further away from the excitation point.

## 8 CORRELATION IN CASE OF DIFFERENT BOUNDARY CONDITIONS

Correlation in case of different boundary conditions (BCs) was evaluated by comparing the natural frequencies and by evaluating both MAC values and COMAC values for selected mode pairs. Comparisons were made between Case 1 and 2 and Case 1 and 3 because there was some interest to find out if there are modes which are not affected by changes in BCs.

Natural mode and frequency comparison shown in Fig. 11 indicates clearly that natural frequencies are highest in Case 3 and lowest in Case 1. This can also be seen in Table 1.

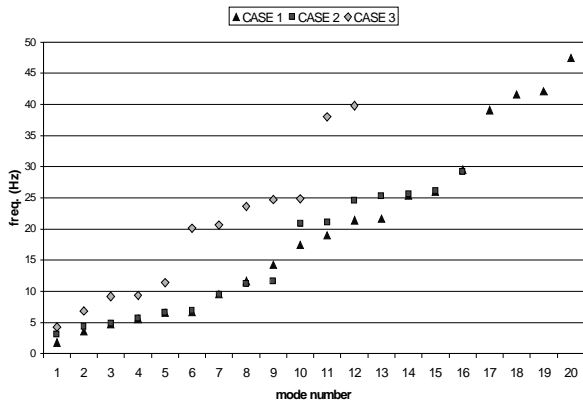


**Figure 11.** Natural mode and frequency comparison of modes below 20 Hz.

### 8.1 Correlation between Case 1 and Case 2

Mode pairs for Case 1 and Case 2 are listed in Table 4 with frequency errors and corresponding MAC values. Mode pairing was made using 20% frequency error and 40% MAC value as pairing criteria.

Mode pairing results show that insulation causes some upward shifting in lower natural modes and some downward shifting in higher modes. This would indicate that insulation causes also increase in stiffness not only increase in mass and damping. The real reason for the impression of increased stiffness is probably due to some contacts, which occur between insulated piping system and some other structures.

One notable fact is that Case 2 modes in mode pair table are mostly running in same order as Case 1 modes, which means that modes with same number are similar at least to some extent. For example mode number 2 from Case 1 and Case 2 have -18.55% frequency difference but they still have a MAC value of 77.5%, which indicates that they have very similar mode shapes (i.e. this mode has shifted upward because of the insulation).

**Table 4.** Mode pairs table for Case 1 and Case 2.

Case 1	Hz	Case 2	Hz	Error	MAC
2	3.59	2	4.41	-18.55	77.5
3	4.72	3	4.92	-4.13	40.9
4	5.60	4	5.67	-1.30	84.9
5	6.55	6	6.93	-5.51	62.2
6	6.68	5	6.63	0.68	86.8
7	9.57	7	9.44	1.38	80.8
8	11.67	9	11.63	0.35	55.6
12	21.40	10	20.91	2.32	53.1
13	21.67	11	21.07	2.87	49.0
15	25.99	12	24.60	5.62	38.3
16	29.54	16	29.22	1.09	81.9

COMAC analysis results in the case of three mode pairs with lowest MAC values obtained from Table 4 are presented in Fig. 12. These results can be used in determining the areas (DOFs) where correlation is good and where correlation is poor. The mode pairs with lowest MAC values were selected for the COMAC analysis in order to study the effects caused by the insulation.

In Fig. 12 higher values (and longer arrows) indicates better correlation and lower values poorer correlation. Here shown is modulus of the COMAC values, which means that all COMAC values (X, Y and Z-direction) are summarised and an ideal maximum value would be 300. COMAC analysis results indicate that with these mode pairs correlation is poorest at the lower part of the piping and at measurement point 113 (see Fig. 4). The former is probably caused by increased mass and damping due to the insulation and latter may be caused by contact between insulated piping and other supporting structure close to the point 113.

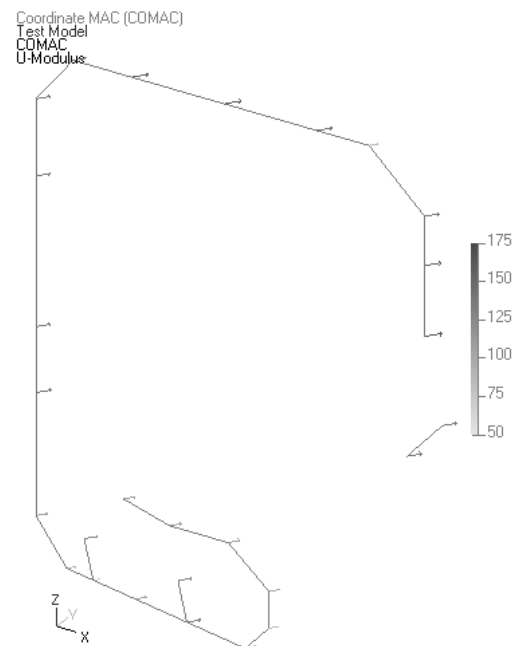


**Figure 12.** COMAC analysis results for three mode pairs with lowest MAC values.

### 8.2 Correlation between Case 1 and Case 3

Mode pairs for Case 1 and Case 3 are shown in table 5 with frequency errors and corresponding MAC values. Mode pairing was made using 20% frequency error and 40% MAC value as pairing criteria.

Mode pairing results shows that insulation together with temperature and water also causes some upward shifting in lower natural modes and some downward shifting in higher modes. With the Case 3 BCs there are much less modes than in Case 1 BCs, but there are still some mode pairs which have very similar mode shapes even if their natural frequencies are different i.e. natural frequency is shifted.

If results in Tables 4 and 5 are compared it can be noted that upward shifting happens in Case 3 only for two first

modes and in general modes in Case 3 have lower frequency than modes in Case 2.

**Table 5.** Mode pairs Case 1 and Case 3.

Case 1	Hz	Case 3	Hz	Error	MAC
2	3.59	1	4.28	-16.02	88.2
6	6.68	2	6.83	-2.25	39.7
7	9.57	4	9.34	2.50	78.9
8	11.67	5	11.43	2.09	65.2
12	21.40	7	20.63	3.71	73.8
14	25.38	9	24.73	2.64	76.6
15	25.99	8	23.64	9.92	43.5
18	41.60	11	37.99	9.49	32.2
19	42.11	12	39.78	5.86	56.4

COMAC analysis results in case of three mode pairs with lowest MAC values from table 5 are presented in Fig. 13. COMAC analysis results indicate that with these mode pairs the correlation is poorest at measurement points 108, 114, 118, 119, 235 and 438 (see Fig. 4).

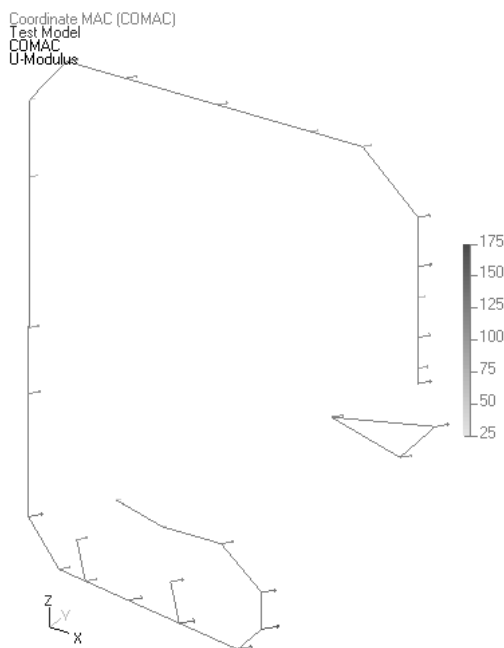


**Figure 13.** COMAC analysis results for three mode pairs with lowest MAC values.

These correlation analysis results indicate that insulation changes the dynamical behaviour of structure significantly especially at frequencies above 20Hz. This is mainly due to increased damping and contacts between insulation and other structures. Addition of heated water to the piping systems does not have very significant effect on the dynamical behaviour.

These results also show that even if boundary conditions change from Case 1 to Case 2 or from Case 1 to Case 3 there are still some modes with similar mode shapes even if natural frequencies are changed. This is

important because these modes could perhaps be used in monitoring changes in actual piping especially if there is an updated FE model available. Also COMAC analysis results could be used for identification of areas with either good or poor correlation from previously selected mode pairs. These mode pairs can of course be selected using different criterions. COMAC analysis results could be used for selecting those DOFs, which are not affected by changed BCs, for monitoring the actual piping.

## 9 CORRELATION BETWEEN SHAKER TEST RESULTS AND OUTPUT-ONLY ANALYSIS RESULTS

Mode pairs for Case 3 BCs with shaker excitation analysis and output only analysis results are shown in Table 6 with frequency errors and corresponding MAC values. Mode pairing was made first for five shaker modes. This table shows that there are at least two good pairs in terms of mode shape correlation (modes 1 and 4) two adequate pairs (modes 3 and 5) and one pair where there is no mode shape correlation (mode 2). With these mode pairs frequency errors are acceptable. It should be remembered that the modal identification in the case of output only analysis was made with the simplest basic FDD technique. The use of some other more sophisticated identification techniques might result to better identified mode shapes. Also it should be remembered that there may have been some differences in the temperatures and that during the output only measurements there was an operational pressure of 7.5 MPa inside the piping.

**Table 6.** Mode pair table for CASE 3 shaker and output only testing results.

shaker	Hz	output	Hz	Error	MAC
1	4.28	1	4.34	-1.49	84.0
2	6.83	2	6.84	-0.15	23.9
3	9.18	3	9.19	-0.13	58.6
4	9.34	4	9.22	1.30	67.2
5	11.43	5	11.66	-1.93	54.8

COMAC analysis results for four mode pairs with highest MAC values found in Table 6 are presented in Fig. 14. Pairs with highest MAC values were now selected because it is obvious that the second mode have low correlation and it would dominate the COMAC analysis results if it would be included. COMAC analysis results indicate that with these mode pairs the correlation is poorest at measurement points from 105 to 110 and points 228 and 438 (see Fig. 4). These results might be improved by using more reference coordinates than one because some of the modes may not have significant contribution to the response at this particular reference point 114Y-.



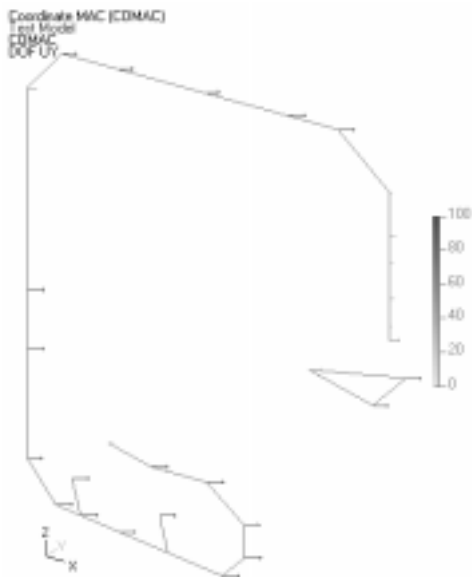


**Figure 14** COMAC analysis results for four mode pairs with highest MAC values.

These preliminary results indicate that the output only modal analysis technique can be utilised in real operational conditions for identifying natural modes with at least some success and their capabilities should be studied even further.

## 10 CONCLUSIONS

Results from impact hammer tests and shaker tests correlated well at lower frequencies even with a massive structure like this. Also, correlation seems to be better in areas closer to the excitation point than in areas further away from the excitation point. This means that impact hammer testing should be very effective in the case of less massive structures and in the case of massive structures impact hammer testing results may be improved by using more than one excitation point.

These correlation analysis results indicate that the dynamical behaviour of the piping was significantly affected by the insulation, especially at frequencies above 20Hz. This is mainly due to the increased damping and contacts between the insulated piping and other structures. Adding heated water to the piping system does not have very significant effect on the dynamical behaviour of the structure.

Correlation analysis results between different cases shows that even if boundary conditions change there can still be found some modes with similar mode shapes even if the natural frequency values are different. In the case of two mode shapes obtained using for example model test results obtained from non-insulated and empty pipe and pipeline in operational conditions are similar then their stiffness and mass distributions can be assumed to be similar. This is important because these modes could perhaps be used in monitoring changes in actual piping, especially if there is an updated FE model available for structural analyses. Also COMAC analysis results could be used for identification of areas with either good or poor correlation from previously selected mode pairs. In order to monitor the actual piping, COMAC analysis results could be further used for

selecting those DOFs, which are not affected by changes in BCs.

These preliminary results from the output only modal analysis indicate that this technique can be used for identifying natural modes from time history measurements made in real operational conditions with at least some success and their capabilities should be studied even further.

In order to evaluate effects of the insulation as well as usefulness of output only modal analysis technique in the case of a piping system with more complex support structures further studies are needed.

## ACKNOWLEDGEMENTS

This presentation was prepared for a joint Finnish industry group as part of a project on Structural Operability and Plant Life Management (RKK). The project funding by the National Technology Agency (Tekes), Teollisuuden Voima Oy (TVO), Fortum Power and Heat Oy, Fortum Energy Solutions Ltd., Fortum Nuclear Services Ltd., FEMdata Ltd., Neste Engineering Ltd., Fortum Oil and Gas Ltd. is gratefully acknowledged. The authors are indebted to Mr Aimo Tuomas and to Mr Timo Krouvi from Fortum Loviisa NPP for their contribution during this work.

## REFERENCES

- [1] FEMtools Theoretical Manual. Version 2.1.0. Dynamic Design Solutions N.V. (DDS). Leuven, Belgium, 2001.
- [2] ABAQUS Theory Manual, Version 5.8. (1998). Hibbit, Karlsson & Sorensen Inc. RI.
- [3] Van Lagenhove, T. & Brughmans, M. Using MSC/Nastran and LMS/Pretest to find an optimal sensor placement for modal identification and correlation of aerospace structures. Presented at the 2nd MSC Aerospace Conference, June 1999. 12p.
- [4] Nurkkala, P. Loviisa 1 syöttövesilinjan painepuolen RL61 putkiston moodianalyysi kolmella eri reunaehdolla elokuussa ja lokakuussa 2001. Fortum CMC. Työseloste CMC-201 to be published.
- [5] I-DEAS Test. Modal Analysis User's Guide. I-DEAS Master Series 7 (1998). Structural Dynamics Research Corporation. USA.
- [6] Rostedt, J. Fortum Power and Heat Oy, Loviisa Power Plant-MODAL ANALYSIS OF PIPELINE RL-61 USING HAMMER EXCITATION. Research Report 020301.doc, J. Rostedt Ltd, Kankaanpää, Finland, 2002.
- [7] ARTeMIS Extractor Getting Started Manual For all versions. Structural Vibration Solutions ApS. Aalborg, Denmark.
- [8] Brinker, R., Zhang, L. and Andersen P. Output-Only Analysis by Frequency Domain Decomposition. Proceedings of ISMA 25, Vol 2, 2000.
- [9] Ewins, D. J. Modal Testing: Theory and Practice, Research Studies Press Ltd. Letchworth, Herts, U.K, ISBN 0-86380-036-X, 269 p. 1986.
- [10] Imregun, M., Visser, W. J. & Ewins, D. J. Finite element model updating using frequency response function data - I. Theory and initial investigation. Mechanical Systems and Signal Processing (1995) 9(2), Pp. 187 - 202.